energies

MDPI

Article

Controls on Reservoirs Quality of the Upper Jurassic Mengyin Formation Sandstones in Dongying Depression, Bohai Bay Basin, Eastern China

Shaochun Yang [1,2,*], Ya Wang [1,2,*], Shiqi Zhang [1,2], Yongchao Wang [1,2], Yifan Zhang [1,2] and Yongfu Zhao [1,3]

[1] School of Geosciences in China University of Petroleum, Qingdao 266580, China; shqzhang@upc.edu.cn (S.Z.); wych1992@163.com (Y.W.); b18010037@s.upc.edu.cn (Y.Z.); b14010036@s.upc.edu.cn (Y.Z.)
[2] Key Laboratory of Deep Oil and Gas, China University of Petroleum (East China), Qingdao 266580, China
[3] Management Center of Oil and Gas Exploration, SINOPEC Shengli Oilfield, Dongying 257017, China
* Correspondence: scyang@upc.edu.cn (S.Y.); wangyayifan@163.com (Y.W.); Tel.: +86-532-8698-1889

Received: 10 January 2020; Accepted: 30 January 2020; Published: 3 February 2020

Abstract: The Upper Jurassic Mengyin Formation sandstones are important targets for petroleum exploration in Dongying Depression of Bohai Bay Basin, Eastern China. Although the current burial depth of the Upper Jurassic Mengyin Formation sandstones is shallow (900–2500 m), the reservoir rocks are characterized by low porosity and low permeability due to the complex diagenetic modifications after deposition. Experimental tests and statistical methods, such as thin section, scanning electron microscopy (SEM), cathodoluminescence (CL), high pressure mercury injection (HPMI) and fluid inclusion analysis are conducted to delineate the mineralogical, petrographic and petro-physical characteristics. Results show that physical and chemical processes, including burial depth, burial and thermal history and pore fluid evolution, are both important for the diagenetic modifications that result in a variety changes in pore system and reservoir quality. According to numerical simulation of porosity evolution during lengthy burial and thermal history, porosity loss due to the early deep burial process under the high paleo-geothermal gradient can reach about 20%. Moreover, the burial history (effective stress and temperature) has a better guidance to reservoir quality prediction compared with current burial depth. The extensive compaction in sandstones also resulted in extremely low pore fluid flow during subsequent diagenetic processes, thus, the reaction products of dissolution cannot be removed, which would be precipitated as carbonate cements during stable reburial phase. Dissolution resulted from uncomformity-related meteoric flushing have been the most important porosity-enhancing factor in Mengyin Formation sandstones in spite of low thin section porosity averaged out to 3.22%. Secondary pores derived from dissolution of unstable silicates are more likely to develop in sandstones near the regional unconformity. The oil source fault activities may enhance the heterogeneity of reservoir rocks and control the reservoir quality by inducing micro-fractures and providing the main pathways for hydrocarbon migration.

Keywords: reservoir quality; diagenesis; numerical simulation; uncomformity; meteoric flushing

1. Introduction

Reservoir quality is one of the important factors to control hydrocarbon accumulation and recovery efficiency [1–6]. Investigation of the controls on reservoir quality are of great importance for prediction of reservoir heterogeneity and management of oil and gas recovery. Significant efforts have been focused on the controlling factors of reservoir quality [7–13]. These studies confirmed that the initial sedimentary settings, diagenetic modifications and tectonic activities are the primary

factors controlling reservoir quality and pore system evolution, and the interplay between these factors can induce various extents and scales of reservoir heterogeneities in sandstones.

The heterogeneous spatial distribution of petrophysical properties within sand bodies, including porosity, permeability, density, water/hydrocarbon saturation and lithology, are believed to be highly related to sedimentary settings [9,14,15]. The variations in sedimentary settings, including mainly framework grains compositions, sorting, grain size and pore water chemistry, have a profound impact on chemical and mechanical stability and burial diagenetic pathways of sandstones, which in turn control the pore system and reservoir quality evolution [9]. Diagenetic alterations are believed to enhance the heterogeneity to various extents in sandstones [15]. Diagenetic processes of compaction, cementation and dissolution are the dominated porosity reducing/preserving/enhancing factors, respectively, which significantly alter the petrophysical properties of the reservoir rocks to various extents [16]. The coexistence of multi-type and multi-scale pores in sandstones are largely the results of various diagenetic modifications [15,17,18]. Paleogeotemperature has been confirmed to play a key role in diagenetic alterations, which exerted strong control on degree of compaction, conversion of clays, pressure dissolution and quartz cementation [9,19–21]. The increasing compaction degree with burial depth and paleogeotemperature contributed to rapid loss of original porosity. Occurrence time and duration of deep burial largely control the preservation of pores and reservoir quality [22,23]. The negative effects on reservoir quality by compaction may be inhibited by eogenetic cements such as extensive carbonate cements [17,24]. Porosity enhancing factors, including mainly dissolution of unstable silicate and fracturing, depend crucially on pore fluid chemistry, grain compositions, and structural features (development of fractures, e.g., joints and faults) [19,25,26]. Regional uncomformity commonly indicates prolonged weathering and erosion of strata, long duration of meteoric water flushing and percolation and extensive dissolution and kaolinization of unstable silicates in reservoir rocks, which would greatly promote the formation of secondary porosity in many cases [27–29]. Consequently, the reservoir quality evolution is controlled by a variety of the above mentioned physical and chemical factors. Therefore, the investigation and understanding of these factors are of great importance during the exploration and development of oil and gas fields.

The work presented in this paper focuses on the Jurassic Mengyin Formation (J_3m) in the Gaoqing area, aiming to provide insight into the framework constituents, diagenetic features, macroscopic petrophysical properties and pore systems. Moreover, the impacts of compaction, unconformity and fractures on reservoir quality are investigated using integrated methods, including thin sections, cathodeluminescence, scanning electron microscopy, fluid inclusion analysis and high pressure mercury injection.

2. Geological Setting

2.1. Regional Geology

The Bohai Bay Basin is one of the most important hydrocarbon provinces in East China [10,30–32]. The Dongying Depression, located on south-eastern part of Bohai Bay Basin (Figure 1A), is about 90 km long in an East-West direction and 65 km wide in a North-South direction, containing extensive hydrocarbon accumulations [33] (Figure 1B). The Gaoqing area at the south-west part of Dongying Depression, consisting of southern uplift and northern slope (Figure 1C), is bounded by Gaoqing fault with an exploration area of approximately 350 km^2. The dark shale rich in organic matter from Shahejie Formation (Es) in adjacent Boxing Sag, located at the downthrown side of the Gaoqing fault, have provided abundant hydrocarbon sources [34]. The organic carbon contents of the Shahejie Formation (Es) source rocks are in the range of 1.5%~3%, with potential of generating hydrocarbon between 16–20 mg/g [34]. Two periods of hydrocarbon generation and expulsion of these source rocks have been confirmed [34]. Multi-oil-bearing series and multi-reservoir types have been found in the Gaoqing area, which is the target area of this study.

As a boundary between the Gaoqing area and Boxing Sag in the east of the study area, the Gaoqing fault is a long-term active basement normal fault and it largely controls the structural

features of study area [35]. The Gaoqing fault has been active since the late Cretaceous, and the intensity of fault activity reached a peak in Paleogene. The strata in Gaoqing area was uplifted due to the fault activity, which resulted in the formation of Qingcheng Bulge (Figure 2), and the Upper Jurassic strata was subjected to prolonged erosion and weathering since the late Cretaceous [22,23]. The activity of Gaoing fault caused the formation of several unconformities in Gaoqing area from Jurassic to Paleogene, among which the uplift in the late Paleogene period (approximately 24Ma-22Ma) contributed to the formation of a regional unconformity between Ng Formation and the underlying layers (Figure 1C). The Gaoqing fault and its secondary faults are considered to acts as the important vertical migration pathways for the long-distance migration of oil and gas in this area, which profoundly influence the distribution of oil and gas [36].

2.2. Stratigraphy and Depositional Facies

According to the wells (well G41, G54, G56 and G59) drilling, the sediments deposited in the Gaoqing area are characterized by the Archean Taishan group, Lower Paleozoic Cambrian and Ordovician system, Upper Paleozoic Carboniferous and Permian system, Mesozoic Jurassic and Lower Cretaceous system, Cenozoic Paleogene, Neogene and the overlying Quaternary system, from base to top. In the southern uplift, since the coarse clastic rocks underlying the Neogene Guantao (Ng) Formation were eroded, the Neogene dominated by mudstones directly cover the different layers of Mesozoic.

The Jurassic Mengyin Formation (J_3m) in the Gaoqing area are important hydrocarbon producing layers, with current burial depth reaching up to 900-2500m. During the deposition of the Mengyin Formation (J_3m), the braided delta front deposition was widely developed in the low accommodation space due to the semi-arid-humid climate in the Gaoqing area [37]. The braided rivers channel sand bodies were characterized by poor lateral continuity and high degree of mutual cutting. The deposits of Mengyin Formation (J_3m) are dominated by greyish fine-grained sandstones with interbedded mudstones or siltstones (Figure 1D).

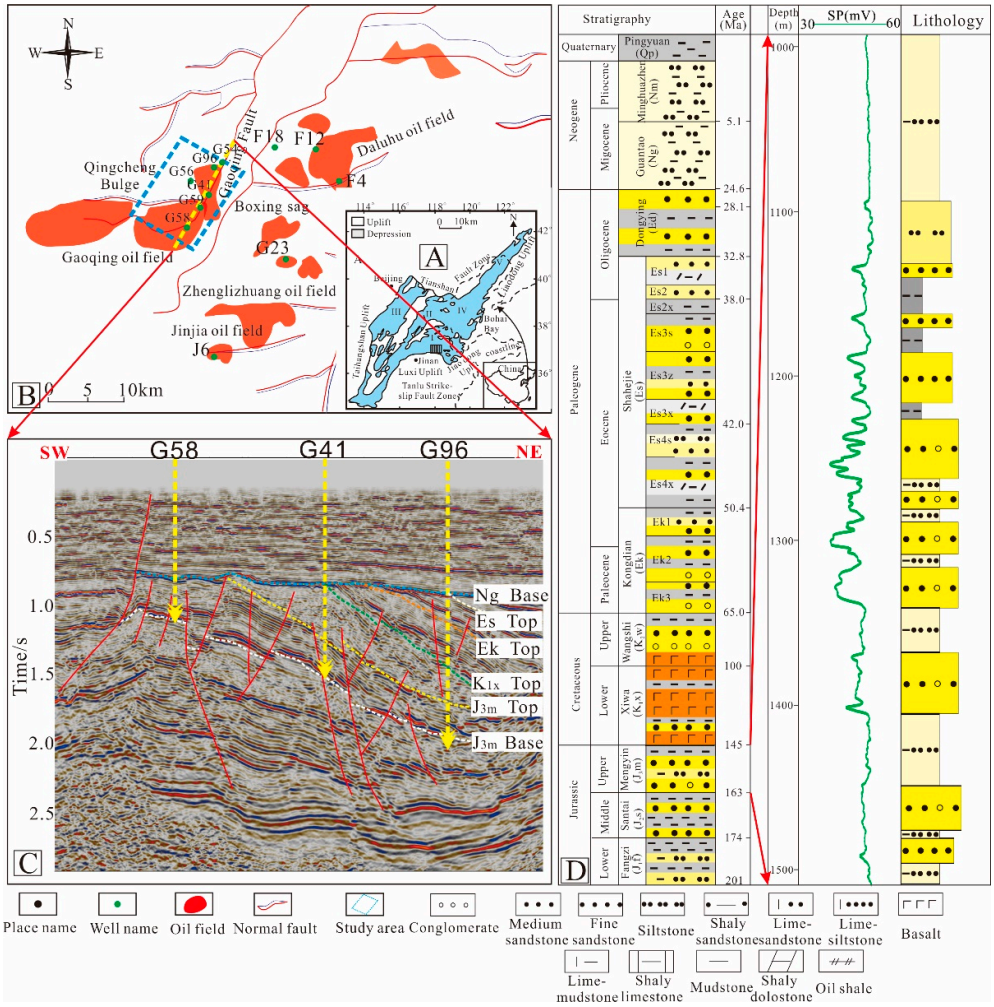

Figure.1 Structural location of study area (B) in the Bohai Bay Basin (A), China; Seismic section showing the structural features of study area (C); Generalized Jurassic-Quaternary stratigraphy column of the Dongying Depression (D).

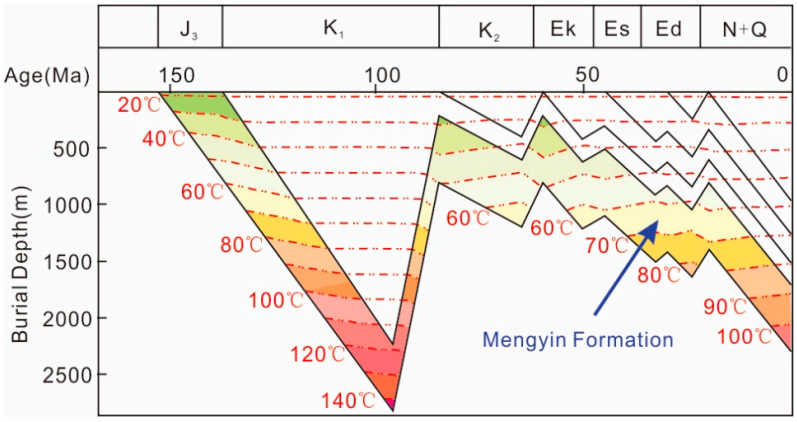

Figure 2. One-dimensional (1D) burial history and geotemperature history model in the Upper Jurassic Mengyin Formation of well G41.

3. Material and Methods

All the samples examined in this study were collected from the cored intervals of the Upper Jurassic Mengyin Formation in the Gaoqing area. Four wells (well G41, G54, G56 and G59) were selected for various core-based measurements due to their availability and accessibility of cores.

Routine rock properties measurements, including helium porosity and air permeability analysis, were conducted on 465 core samples with 2.54 cm in diameter and 5 cm in length to reveal macroscopic petrophysical properties of reservoir rocks.

In total, there were 151 core samples with blue epoxy resin to highlight porosity and stained with Alizarin Red S and potassium ferricyanide for the simple recognition of carbonate minerals (dolomites, ferroan calcite and nonferroan calcite). The amounts of detrital and diagenetic components, porosity and pore types, as well as intergranular volume, were determined by point-counting (at least 300 points per slide). Thin sections were photographed using a Leitz incident light microscope to take digital measurements of mean grain size, grain sorting and grain roundness.

Cathodoluminescence (CL) analysis of 20 polished thin sections were conducted using a Technosyn cold cathode luminoscope with the acceleration voltage of 20 kV, 200e400 mA to provide insights into cementation, grains and timing of cementation [38]. Twenty core samples were selected for scanning electron microscope (SEM) to confirm the clay minerals types, petrography texture and to determine the pore structure.

Fluid inclusion microthermometry was performed on 44 samples using an Axio Imager D1m microscope attached to a LinkhamTHM600 heating-freezing stage (minimum trapping temperatures and salinities), using the ice melting/salinity conversion tables of Bodnar (1993) [39].

High Pressure Mercury Injection (HPMI) was conducted on 39 core plug samples (2.5 cm in diameter and 1 cm in length). A mercury porosimeter was used to generate pressure high enough (163.82 MPa, 23758.62 Psi) to force the mercury into interconnected pores larger than 0.004489 μm.

Numerical modelling was served to simulate the porosity evolution using PetroMod software (version 2012) by considering the compaction, thermal and effective stress history of sandstones. The model was calibrated to match present reservoir properties (porosity and permeability) using routine core analysis data.

4. Results

4.1. Mineralogical Composition and Textures of Sandstones

The studied types of rocks are classified as sandstones with a clastic texture. They are mainly categorized as lithic arkose and rarely feldspar litharenite subarkose (Figure 3 and Table 1). Quartz is in the range from 22% to 51%, with an average of 35.74%. The content of feldspar varies from 17% to 44% (average 36.62%) and mainly consists of potassium feldspars and plagioclase feldspars. Rock fragments make up 15–56% (average 27.32%) of the sandstones, consisting mainly of volcanic lithic fragments and metamorphic lithic fragments. Only minor amounts of sedimentary lithic fragments (average 1.45%) can be observed in the sandstones.

The median grain sizes of the samples from Mengyin Formation ranges from clay to coarse sand (Table 2). The majority of the samples comprise silty to medium sandstones (Table 2). The sediments are mainly of finer grain size with an average median grain size of 198 μm. The sandstones are moderately to poorly sorted.

Table 1. The compositions of Mengyin Formation sandstones samples in the Gaoqing area.

Component	Min	Max	Average
Detrital grains			
Quartz (vol. %)	22	51	36
Potassium feldspars (vol. %)	10	25	17
Plagioclase feldspars (vol. %)	5	30	19
Total of rock fragments (vol. %)	15	56	27

Volcanic lithic fragments (vol. %)	5	30	13
Metamorphic lithic fragments (vol. %)	2	26	13
Sedimentary lithic fragments (vol. %)	1	13	1
Mica (vol. %)	0	2	0
Chert (vol. %)	0	3	0
Matrix (vol. %)	0	40	6
Diagenetic components			
Calcite (vol. %)	0	25	3
Ferroan-calcite (vol. %)	0	28	3
Dolomite (vol. %)	0	2	0
Ferroan-dolomite (vol. %)	0	7	0
Quartz overgrowths (vol. %)	0	1.5	0
Clay minerals (vol. %)	4	23	8
Porosity			
Primary porosity (vol. %)	0	8.23	1
Secondary porosity (vol. %)	0	14.24	3

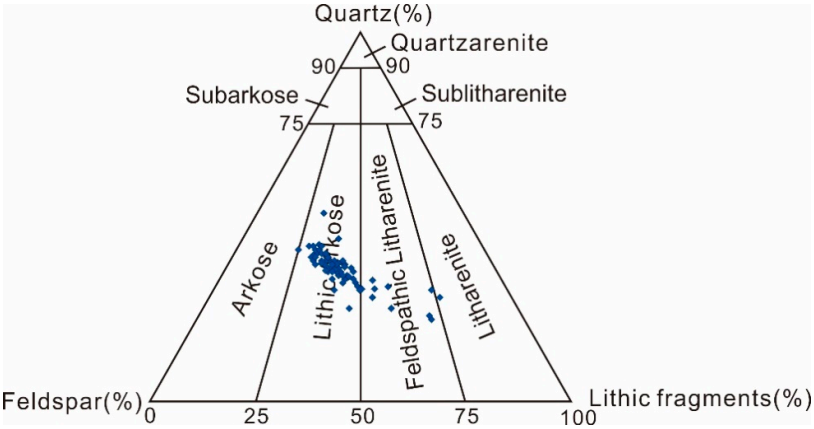

Figure 3. Triangle classification diagram of rock types in the J3m clastic reservoir in Gaoqing area (after Folk, 1968) [40]. Q: quartz; F: feldspar; L: Rock fragments.

Table 2. Grain compositions and characteristics of J3m sandstones in the study area.

Grain grade	Min	Max	Ave
Coarse sand (%)	0	20.6	4.77
Medium sand (%)	0	27.4	23.38
Fine sand (%)	0	26.3	38.33
Silty sand (%)	0	40	26.47
Clay (%)	1	36	7.05
Medium grain size (μm)	50	690	198
Sorting coefficient	1.31	3.93	1.71

4.2. Petrographic Features and Diagenesis

4.2.1. Compaction

According to the petrographic analysis of thin sections and scanning electron microscopy (SEM), evidences indicative of strong compaction in the sandstones are abundant, including orientation of detrital particles, long contacts, bending of mica and fracturing of detrital grains (Figure 4A,B,E). The ductile rock fragments are generally deformed and sometimes squeezed to pseudomatrix between rigid grains, destroying the original porosity significantly. The pressure dissolution and quartz

overgrowth along the contacts of detrital quartz grains can be also observed, which are evidences of chemical compaction of deep buried sandstones (Figure 4D,F). The compaction degree in Mengyin Formation sandstones is strong in most of the samples, while in a few fine-grained sandstone samples adjacent to the regional uncomformity compaction is limited due to pervasively eogenetic carbonate cementation (Figure 4C).

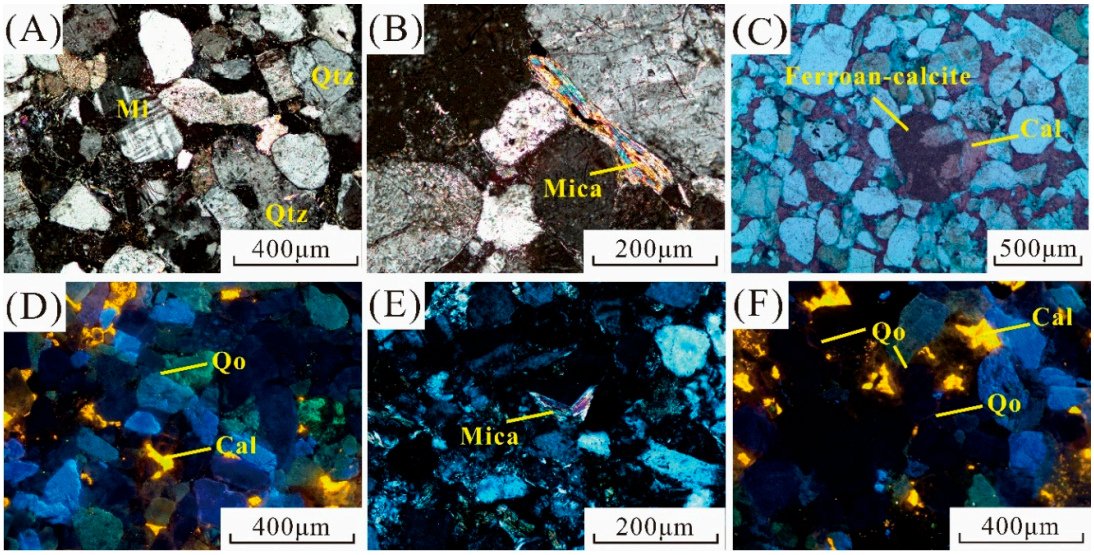

Figure.4. (A) Photomicrograph of long contacts between detrital grains and ductile deformation of rock fragments from well G59 at 1009.1 m (XPL); (B) Photomicrograph of planar contacts between quartz grains and muscovite from well G54 at 2103.5m (XPL); (C) Photomicrograph of pore-filling calcite from well G41 at 1321.68 m (PPL); (D) Cathodoluminescence (CL) image of long contacts and quartz overgrowth from well G54 at 2105.0 m; (E) Photomicrograph of fracturing of mica and ductile deformation of rock fragments from G41 at 1321.68 m (XPL); (F) Cathodoluminescence (CL) image of long contacts and quartz overgrowth from well G41 at 1254.21 m. Qtz-quartz, Cal-calcite, Qo-quartz overgrowth, Mi-microcline, (PPL) and (XPL) indicate the parallel polarized light and cross polarized light, respectively.

4.2.2. Cementation

The cementation in reservoir rocks of Mengyin Formation is complex and diverse, including carbonates, quartz and authigenic clay minerals.

Carbonate cements are common in reservoirs rocks of the Mengyin Formation, and there are three stages of cementation according to petrographic analysis of thin sections and cathode luminescence (Figure 4C and Figure 5A–C). The early stage of carbonates mainly occurred as calcite and dolomite cements, and the mechanical compaction is limited due to the increase in pressure-resistance (Figure 5A), which suggests the calcite and dolomite cements was eogenetic (pre-compactional) in origin. Early stage carbonate cements are generally completely or partially dissolved, so very little remains in the sandstone. The mid stage of carbonates occurred as pore-filling calcite (0–22.2, average 3.01%), which is the most abundant cement in Mengyin Formation sandstones of the study area (Figure 4D and F; Figure 5B and C). The late stage of carbonates occurred as scattered patchy ferroan-calcite and ferroan-dolomite, or forms overgrowths on corroded or replaced calcite and dolomite cement and thereby post-dates the mid-stage calcite cement (Figure 4C and Figure 5C).

Quartz cements occur only sporadically, generally as euhedral, syntaxial overgrowths around detrital quartz grains supported by thin sections, CL and SEM images (Figure 4D and F; Figure 5C and D). Authigenic quartz microcrystals also grows into dissolved pores, including intragranular K-feldspar dissolved pores and intergranular dissolved pores, which suggest that the material source of quartz microcrystals may be derived from dissolution of K-feldspar.

The constituents of clay minerals are kaolinite, illite, smectite and illite/smectite mixed layers. Kaolinite mainly occurs as clusters of pore-filling small booklets accompanied by dissolution (Figure 5F). In the SEM, illite commonly grows on the surface of quartz particles and occurs as honeycomb texture, suggesting that authigenic smectite was diagenetically altered into fibrous illite (Figure 5E). The fibrous illite, growing on detrital grains, constituted pore-lining and bridges pores between individual grains which increased throat curvature and deteriorated reservoir quality, especially permeability. Illite/smectite mixed layers are ubiquitous in the sandstones, growing around the detrital grains.

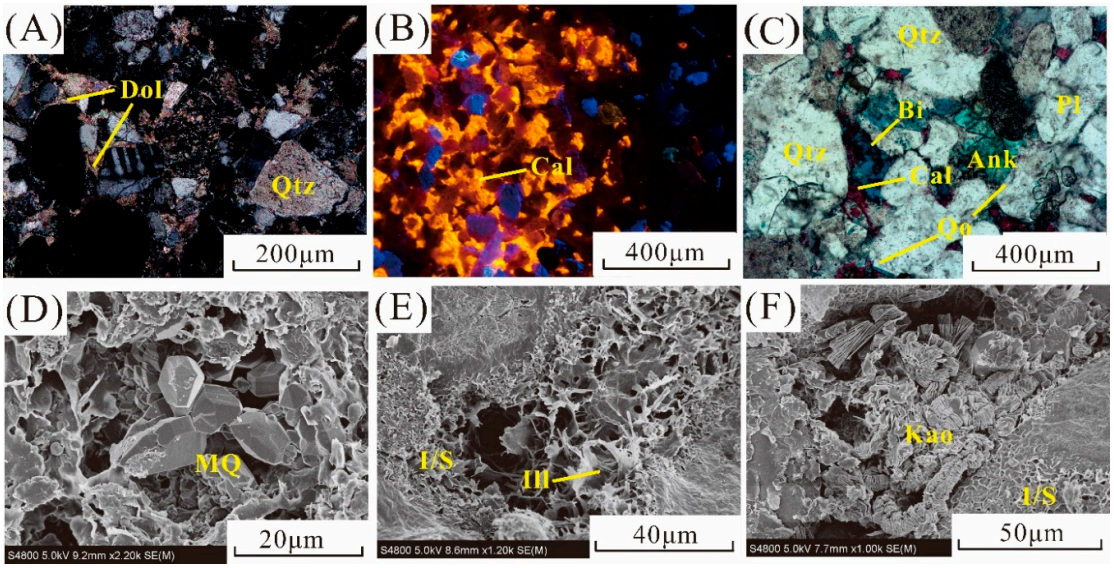

Figure 5. (A) Photomicrograph of dolomites filling in intergranular pores from well G41 at 1243.8m (XPL); (B) Cathodoluminescence (CL) image of microcrystalline calcite filling large intergranular pores between loosely packed framework grains and replacing the framework grains (mainly feldspars) from well G41 at 1326.44 m; (C) Photomicrograph of dissolved pores with black edge of bitumen and ankerite occurring as replaced dolomite from well G41 at 1240.16 m (PPL); (D) SEM images of authigenic euhedral and syntaxial quartz in secondary pores from well G41 at 1218.68 m; (E) SEM images of fibrous illite showing honeycomb texture from well G59 at 1517.9 m; (F) SEM images of pore-filling kaolinite aggregates from well G41 1280.45 m. Qtz-quartz, Dol-dolomite, Cal-calcite, Qo-quartz overgrowth, Ank-ankerite, Pl-plagioclase, MQ-microcrystalline quartz; Kao-kaolinite, Ill-illitite, I/S-illite-smectite mixed layers, Bi-bitumen, (PPL) and (XPL) indicate the parallel polarized light and cross polarized light, respectively.

4.2.3. Dissolution

Diagenetic features of dissolution are frequently detected under microscopic observations, forming high abundance of secondary dissolved pores with various types and geometries (Figure 6A–F). The secondary dissolved pores make up more than 85% of the total pore volume. Moreover, the constituents of secondary dissolved pores are intragranular dissolved pores of chemically unstable grains and intergranular dissolved pores of carbonate cements. Feldspars are commonly dissolved along the grain edges or cleavage surfaces, forming large amounts of intragranular pores or even moldic pores (Figure 6B,C). The extensive dissolution of feldspars is especially frequent in feldspar-rich sandstones under unconformity and it is the main contributor of secondary porosity. Extensive dissolution of detrital grains and carbonated cements related with micro-fractures occurred occasionally in sandstones (Figure 6E,F). This indicates that the micro-fractures can promote dissolution and contribute a significant improvement to reservoir quality.

In general, the modification of dissolution would significantly broad ranges of pore throats size distribution, reshape pore structure and improve connectivity of pore system, and therefore, is an important porosity-enhancing factor in Mengyin Formation sandstones.

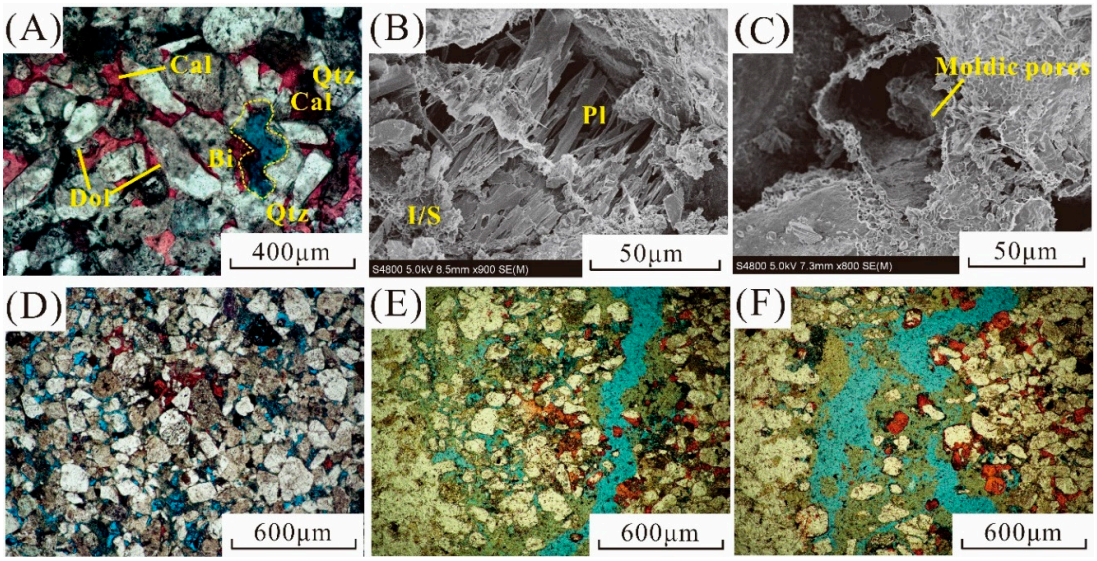

Figure 6. (A) Photomicrograph of dissolution of pore-filling calcite and secondary pores with black edge of bitumen from G41 at 1325.64 m (PPL); (B) SEM images of dissolution of plagioclase along its cleavage from well G56 at 938.5 m; (C) SEM images of moldic pores derived from feldspar dissolution from well G41 at 1280.45m; (D) Photomicrograph of residual pores and dissolved pores with black edge of bitumen from well G56 at 951.82 m (PPL); (E) Photomicrograph of dissolution of micro-fracture related dissolution of detrital grains and cements from G41 at 1264.74 m (PPL); (F) Photomicrograph of dissolution of micro-fracture related dissolution of detrital grains and cements from well G41 at 1264.74 m (PPL). Qtz-quartz, Pl-plagioclase, Cal-calcite, Dol-dolomite, I/S-illite-smectite mixed layers, Bi-bitumen, (PPL) indicates the parallel polarized light.

4.3. Macroscopic Petrophysical Properties

The reservoir rocks of the Mengyin Formation in the study area are characterized by "shallow burial and low porosity", that is, the current burial depth is relatively shallow (900–2500 m), but the physical property is of low porosity and low permeability according to the routine rock properties measurements. The porosity of the sandstones of the Mengyin Formation ranges from 1% to 35%, with an average of 14.03%, whereas the measured air permeability ranges from 0.01 to 317 mD with an average of 2.93 mD.

The porosity and permeability (on a logarithmic scale) of the Mengyin Formation have a good linear relationship, but there seems to be no obvious difference in poroperm characteristics between different lithology (Figure 7). That is to say, due to diagenetic modification, the sedimentary heterogeneity is weakened, whereas the diagenetic heterogeneity is enhanced.

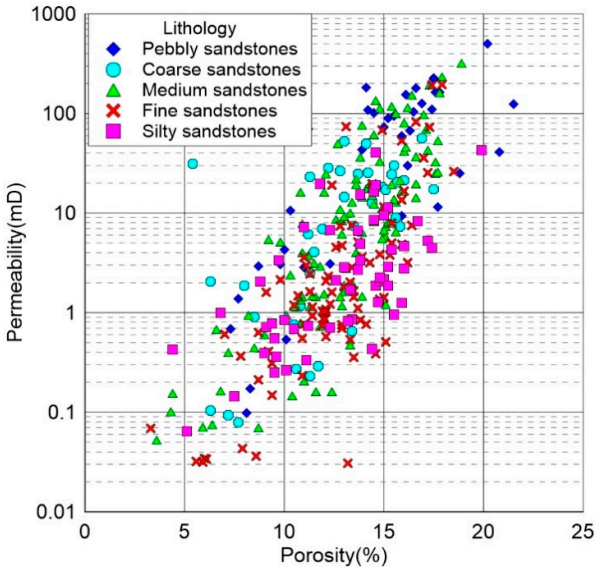

Figure 7. The porosity-permeability relationships of different lithology.

4.4. Pore Systems

The microscopic pore structure plays a critical role in pore fluid seepage and enhancing oil recovery [15,41–43]. The microscopic pore structure in the Mengyin Formation sandstones is characterized by strong heterogeneity with large variations in pore and throat size ranging from nano-scale to mm-scale. According to the experimental parameters of high-pressure mercury injection (HPMI), the pore structure of the Mengyin Formation sandstones can be generally divided into four types (Figure 8) and there are marked differences in the size and distribution of various types of pore throats.

To figure out the pore structure characteristics of Mengyin Formation sandstones, the plot of pore throat size distribution and permeability distribution is used to gain insight into the pore size, pore size distribution and contribution to permeability of different pore throats (Figure 8). As can be seen, the micro pore throats (pore throats radius smaller than 0.5 μm) can be detected in the all four kinds of pore structures. This reveals that the micro pore throats are ubiquitous in the sandstones, which is largely related to the pervasive existence of clay minerals or partially dissolved detrital grains [15]. The pore throat distribution of sandstones with favorable reservoir quality (permeability larger than 5 mD), such as type A and type B, exhibit bimodal distribution features (Figure 8). The pore throat radius and pore throat volume of large pore throat in type A are larger than Type B, and the permeability is significantly higher than that of type B. This indicates that the large pore throats profoundly control the permeability and reservoir quality. The pore throats of both type C and D are characterized by single peak distribution, but the type D is mainly composed of small pore throats. According to the contribution to permeability of various pore throats, the smaller pore throats contribute little to permeability. Conversely, the relatively larger pores make a significant contribution to permeability even if they account for a small proportion of the total pore volume. The micro pores are generally believed to be isolated and disconnected (Figure 9c) [44,45], and small pores are connected by narrow neck or pipe shaped throats due to the superposition of strong compaction and carbonate cementation (Figure 9b). Conversely, large pores, mainly consisting of residual primary pores and large dissolved pores, are basically connected by broad throats (Figure 9a) [46,47].

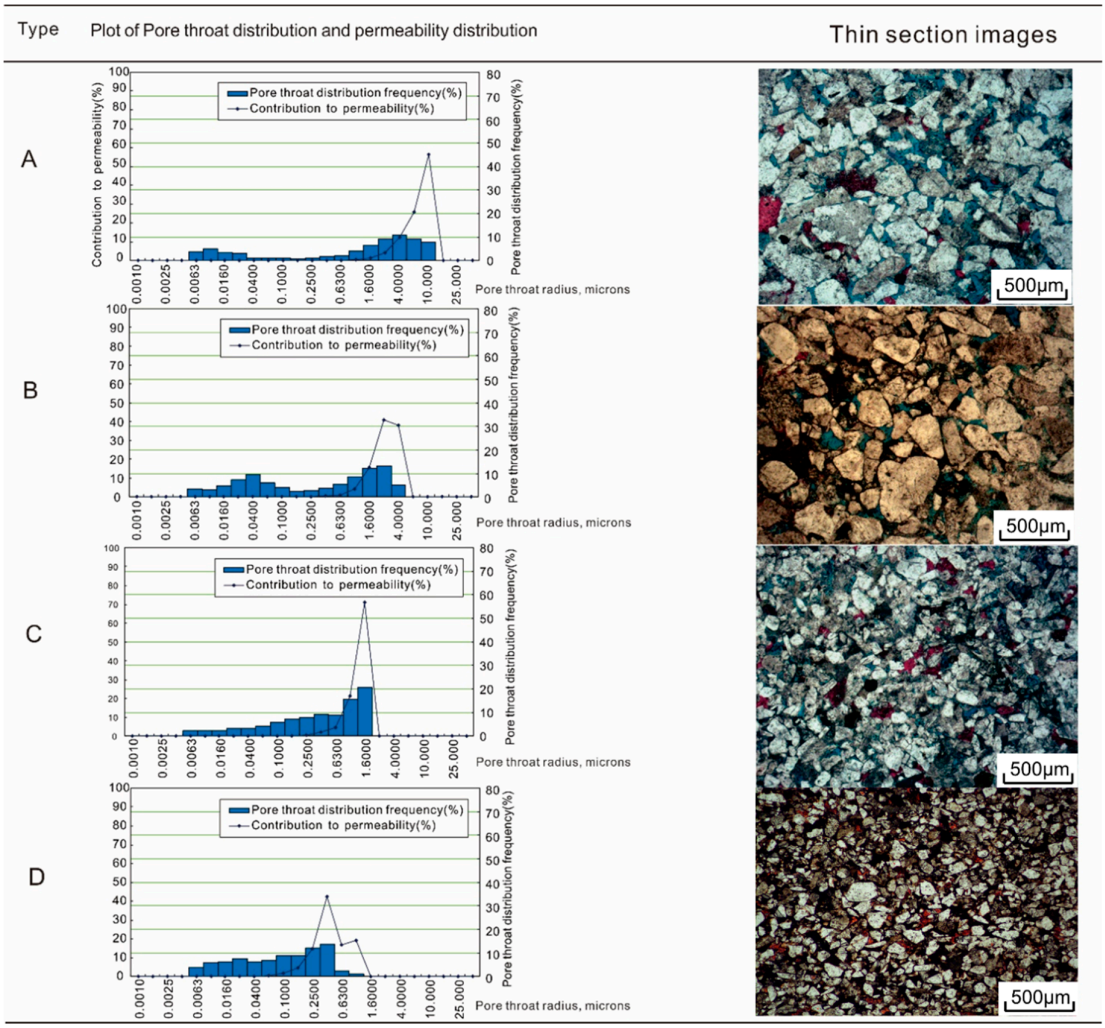

Figure 8. Various kinds of pore structure features obtained from HPMI and petrographic analyses of thin sections. (A) φ=16.2%, K=13.6 mD, r_{max} = 14.13 μm, $r_{average}$=3.75 μm, well G41, 1255.68 m; (B) φ=11.8%, K=6.9 mD, r_{max} = 4.27 μm, $r_{average}$=0.83 μm, well G54, 2104.5 m; (C) φ=17.3%, K=1.04 mD, r_{max} = 2.36 μm, $r_{average}$=0.62 μm, well G56, 952.8 m; (D) φ=10.1%, K=0.02 mD, r_{max} = 0.67 μm, $r_{average}$=0.14 μm, well G59, 1510.1 m.

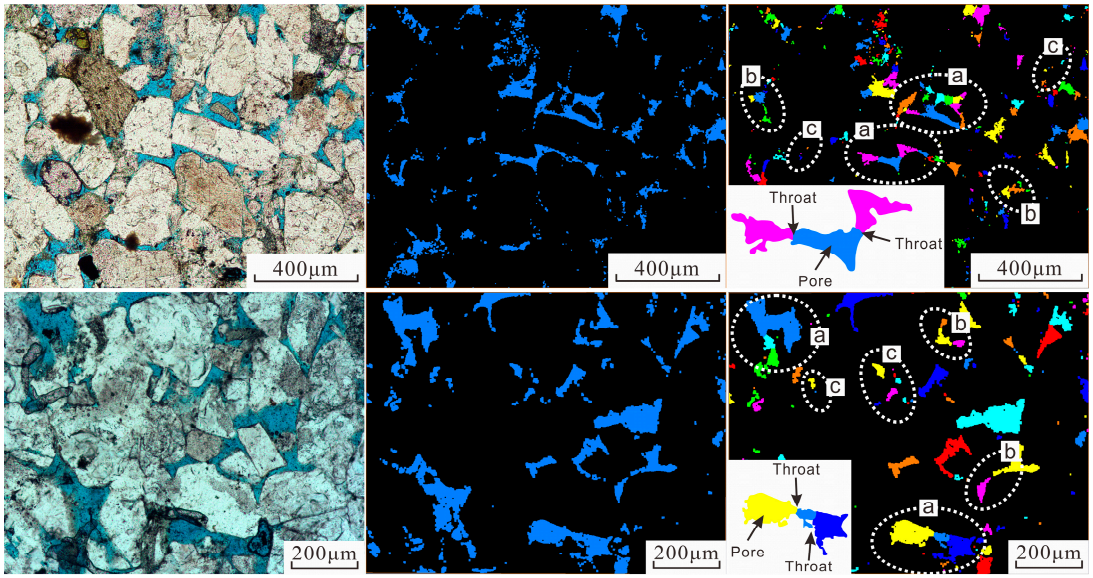

Figure 9. Original photomicrographs of sandstone samples (left), binary images of extracted pore space (middle) and label images of separated pore space (right). (a) Large pores connect by broad throats; (b) Small pores connect by narrow neck or pipe shaped throats; (c) Isolated micro pores.

5. Discussion and Interpretation

5.1. Diagenetic Evolution Sequence

The diagenetic evolution sequence can be broadly related to three important phases in the basin evolution: 1) early burial phase; 2) uplift and meteoric flushing phase; 3) stable reburial phase. These phases are highly influenced by burial pathway and tectonic activities, and variable diagenesis and diagenetic alterations occurred at these phases and induced various patterns and scales of heterogeneity in pore systems and reservoir quality.

5.1.1. Early Burial Phase

The semiarid climate and pore water with high salinity in the Dongying Depression during the Upper Jurassic was favorable for the precipitation of early carbonate cement. Eogenetic carbonate cemented before extensive compaction and could support the rock skeleton, thus, resisting compaction and help to preserve reservoir quality [2] (Figure 9). Moreover, the eogenetic cements can provide material basis for the subsequent dissolution, which is crucial to original pores preservation and dissolved pores development. Early mechanical compaction plays a critical role in reducing the original porosity during the progressive burial, especially in those poorly sorted sandstones with high content of ductile lithic fragments or mudstone matrix. With the increase of burial depth (>2.5 km) and paleogeotemperature (>70 °C), pressure dissolution may be significant enhanced and provide important silica sources for precipitation of subsequent quartz cementation, which would cause severe porosity reduction [48].

5.1.2. Uplift and Meteoric Flushing Phase

The strata of the Gaoqing Area were uplifted and eroded due to the Yanshan movement in the late Cretaceous, thus, the Mengyin Formation entered a prolonged weathering and leaching period (Figure 9). Feldspar and eogenetic carbonate cements were extensively dissolved in those well-sorted sandstones that are characterized by well-preserved primary porosity. The long duration of meteoric water flushing and percolation contributed to significant increase in secondary porosities, thus, broadly enhancing the reservoir quality. The extensive dissolution of chemically unstable silicates may also cause a nearby precipitation of microcrystalline quartz and booklet-like kaolinite aggregates

(Figure 5D and F), both of which will occlude the secondary pore and throats and destroy the reservoir properties [20]. Atmospheric fresh water leaching plays an important role in the development of secondary pores in oil-bearing basins [49], and is a key factor for the improvement of reservoir properties.

5.1.3. Stable Reburial Phase

The chemically unstable minerals would be dissolved in diagenetic environment dominated by organic acid, generating secondary pores with black edge of bitumen. The organic-acid-rich fluids accompanied with the charging of hydrocarbon is suggested to turn the Fe^{3+} generated by the transformation of clays to Fe^{2+} [22]. As the burial depth increased and the organic acid concentration gradually decreased, the Fe^{2+} in the pore fluid may combine with Mg^{2+} and Ca^{2+}, forming late ferroan-calcite and ferroan-dolomite. The ferroan-carbonates generally occurred as replaced calcitic or dolomitic cements in secondary pores with black edge of bitumen and hence have no obvious influence on reservoir quality.

5.1.4. Diagenetic Alteration Relations and Burial History Curve

The tectonic uplift of Gaoqing Area stopped gradually since Neogene, when the sandstones of the Mengyin Formation were stably buried for a second time (Figure 10). In the early reburial phase, with the increase of burial depth and paleogeotemperature, the oversaturated Ca^{2+} generated by the dissolution of feldspar and early carbonate cements precipitated in pores with poor connectivity to form mesogenetic partial to pervasive carbonate cements. The mesogenetic carbonate cements are generally well preserved in the sandstones, only minor cements are dissolved, thus, they cause severe occlusion of pores and throats. The fine-grained sandstones are commonly prone to extensive mesogenetic carbonate cementation, due to the limited fluid flow through rocks. The conversion of smectite formed at low temperature to illite stable at high temperatures during mesodiagenesis may broadly result in reduction of permeability and increase in tortuosity of pore throats [9], since the illite commonly occurred as pore-lining or pore-bridging curving flakes with irregularly ragged edges.

Two episodes of charging and accumulation of hydrocarbon derived from the Shahejie Formation (Es) source rocks can be identified according to the petrographic analysis and homogeneous temperature measurements of fluid inclusion (Figure 11). The homogeneous temperature of brine inclusions accompanied by hydrocarbon organic inclusion ranging from 60 °C to 65 °C indicate the first episode of charging and accumulation of hydrocarbon, corresponding to the Late Paleogene. Furthermore, the second episode of charging and accumulation of hydrocarbon occurred during the Late Neogene, corresponding to the homogeneous temperature of 70–75 °C. However, due to the uplift of the strata caused by the tectonic movement during the Late Paleogene, the hydrocarbon generation process of source rocks was stagnated. Therefore, the oil generation in the first period was limited, and the mudstone cap layer of the Guantao Formation (Ng) had not been formed at this time, thus, it was difficult to accumulate large scale reservoirs. The formation of oil reservoirs in the Gaoqing Area were mainly attributed to the second period of charging and accumulation of hydrocarbon.

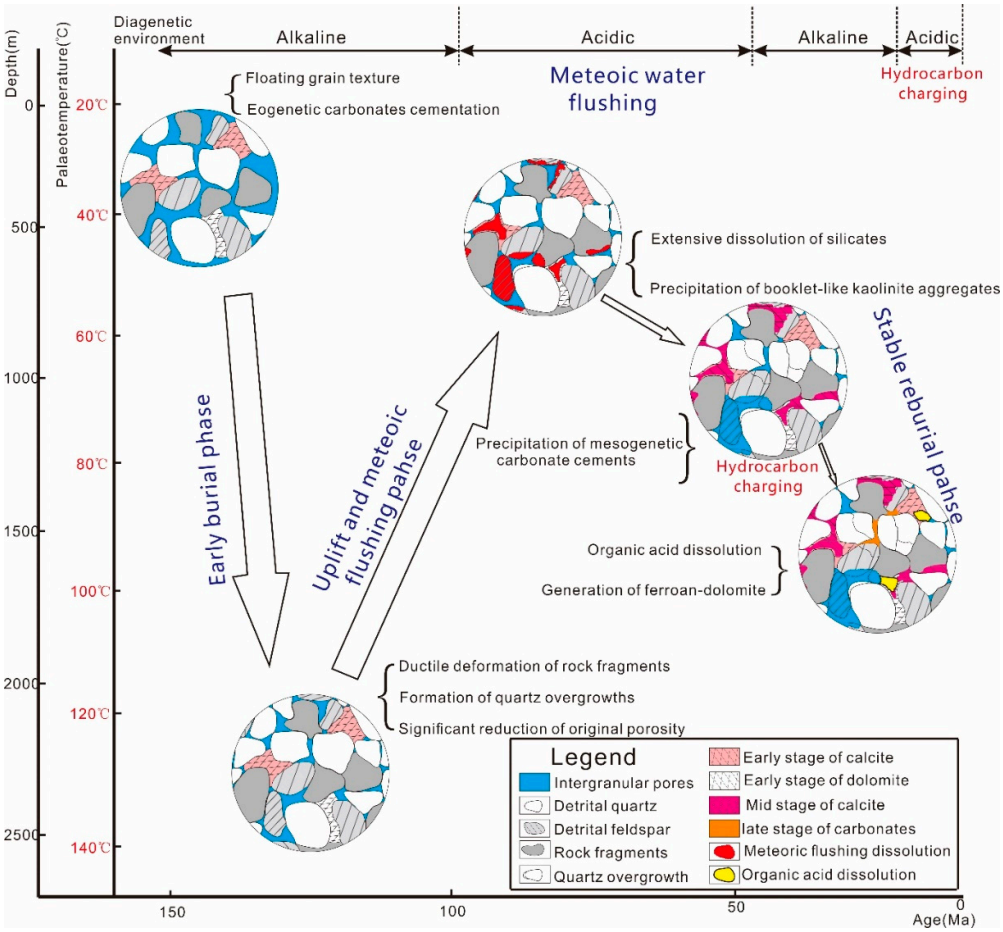

Figure 10. Paragenetic sequence of the diagenetic minerals and alterations in the Mengyin Formation in the Gaoqing area based on diagenetic alteration relations and burial history curve.

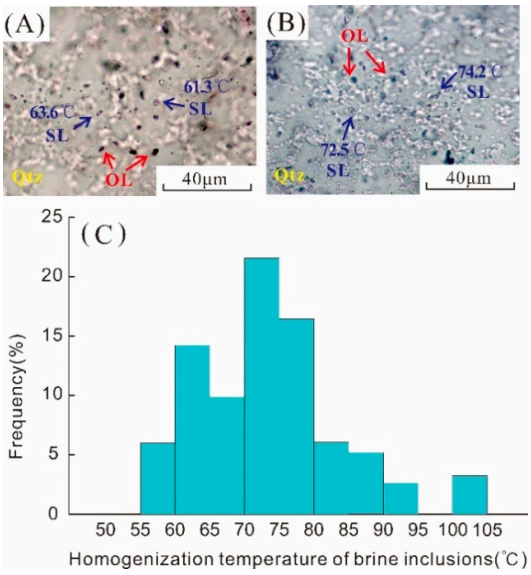

Figure 11. (A) Photomicrograph of brine and hydrocarbon inclusions in micro fractures of quartz from well G41 at 1551.0 m; (B) Photomicrograph of brine and hydrocarbon inclusions in micro fractures of quartz from well G56 at 955.82 m; (C) Homogenization temperature distributions of brine inclusions.

5.2. Relationship between Compaction and Porosity under High Geothermal Gradient

The permeability in Mengyin Formation sandstones is mainly controlled by the relatively large pores. Therefore, the preservation of the primary pores after the compaction and cementation processes and the generation of secondary pores are the key controlling factors for the reservoir properties. Compaction, including mechanical and chemical compaction, has been considered as the most profound factors in reducing primary porosity during the early diagenetic stage [9,21,44]. The diagram introduced by Houseknecht (1987) [50], which plots cement percentage versus intergranular volume (IGV) percentage, can be served to investigate the relative contribution of compaction and cementation to porosity loss. The intergranular volume in the study area is in the range of 1.02–31.49%, with an average of 8.61%. The diagram indicates that compaction is more important than cementation in reducing porosity, with the exception of a few fine-grained samples (Figure 12). These fine-grained sandstone samples are mostly adjacent to mudstones and the regional uncomformity, carbonates were extensively cemented, which may be the precipitation of over-saturated Ca^{2+} derived from extensive dissolution of silicates or discharged from nearby mudstone during compaction.

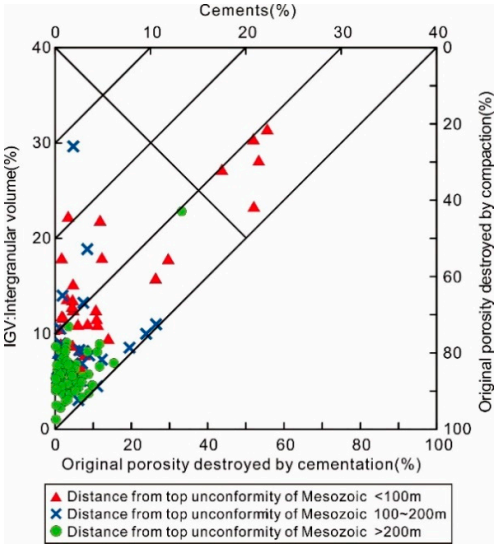

Figure 12. Plot of cement volume versus intergranular volume.

Compaction plays a critical role in pore loss of Mengyin Formation sandstones due to the high geothermal gradient in Bohai Bay Basin, which may reach 4.04–5.25 °C/100 m in Mesozoic. The geothermal gradient greatly influenced the pressure-resistance ability of sandstones by controlling the buried palaeogeothermal. With the increase of paleogeothermal temperature, rocks are more likely to suffer ductile deformation during burial process, thus, undergoing more intense porosity reduction.

In order to figure out how compaction influences porosity during the long burial history, the pore evolution process is simulated based on one-dimensional (1D) thermal history modeling module of Petromod 2012. The original porosity of sandstone has a good correlation with the separation coefficient [51], which can be used to calculate the original porosity of sandstone quantitatively. The equation for calculating the original porosity of the model is expressed as Equation 1. The original porosity of the sandstone in Mengyin Formation is calculated as 34.3%:

$$\varphi_0 = 20.91 + 22.90/S_0 \quad (1)$$

where φ_0 is the primary porosity of sandstones and S_0 is the sorting coefficient of detrital grains.

The 1D model can be used to simulate the residual porosity evolution during the burial history of the sandstones [52]. Moreover, the present-day reservoirs quality is used to optimize the model parameters [53]. Results show that the deep burial of sandstone occurred during the early Cretaceous, during which the maximum paleotemperature reached up to 140 °C and the thermal compaction

effect was significant. The paleotemperature of the sandstones above 70 °C lasted for 48 Ma, and the paleotemperature above 90 °C lasted for 32 Ma (Figure 2). Although the maximum recovered burial depth of Mengyin Formation is 2700 m, the reservoir rocks have undergone significant thermal exposure (temperature integrated over time) due to the high geothermal gradient and prolonged deep buried time, resulting in significant loss in porosity and permeability during the early burial stage. The pore loss of Mengyin Formation sandstones can reach about 20.2% (Figure 13) according to the simulation results. Additionally, the increasing paleotemperature also induced the pressure dissolution along the contacts between quartz grains and sourced for quartz cement precipitation [9], which enhanced the pore loss during deep buried diagenesis, since the solubility generally increase exponentially with temperature [20,54]. Therefore, under the background of high paleogeothermal gradient, the early burial process of deep burial is the main cause of low porosity. The early stage of pore structure of low porosity resulted in a relatively closed water-rock reaction system, which had a significant influence on the subsequent diagenetic modifications, including cementation and dissolution. The subsequent burial diagenetic alterations were primarily constrained by the extent of fluid flow through the remaining pore system [9]. The flow of pore fluid was partially blocked due to the relative closed diagenetic system. The dissolution reaction degree was weak; moreover, the products of dissolution were difficult to be expelled timely. In the presence of suitable temperature and pH value conditions, the dissolution products tend to be precipitate in pore spaces with relatively closed diagenetic environments, further forming dense cementation layers.

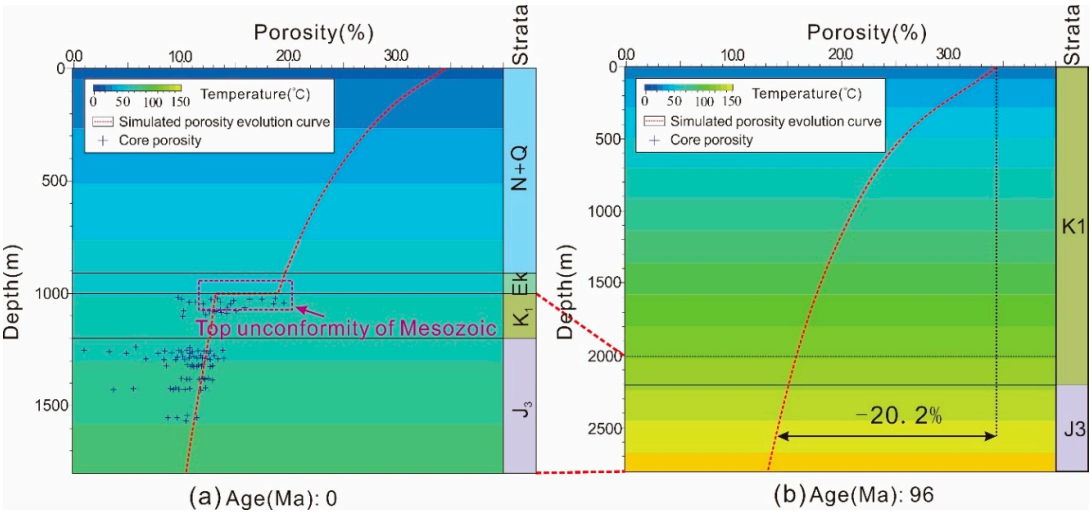

Figure 13. Evolution pathway of pores under thermal compaction in Well G41.

5.3. Uncomformity and Its Effect on the Reservoir Quality

Dissolution is commonly for sandstones influenced by active meteoric water percolation, and is still the most important porosity-enhancing factor in Mengyin Formation. Based on the mechanism of the dissolved pores, the main source of acidic fluids required for dissolution is carbonic acid dissolved in atmospheric fresh water.

The strata of the Gaoqing area were uplifted and eroded due to the Yanshan movement in the late Cretaceous, thus, the Mengyin Formation was subjected to a prolonged weathering and leaching period. The atmospheric fresh water containing CO_2 percolated into pore system of the Mengyin Formation, which caused the dissolution of acid soluble components such as feldspar and carbonate cement. The abundant chemically unstable silicates in Mengyin Formation sandstones, such as feldspar (average 36.62%), are very favorable for the generation of secondary pores. The presence of kaolinite as clusters of small booklets in dissolved pores are largely resulted from dissolved feldspar. Moreover, the authigenic euhedral quartz could be detected under SEM observations, growing into secondary pore space, which is also an evidence of extensive dissolution. According to thin section porosity statistics, the thin section porosity of dissolved pores is negatively correlated with the

distance from top unconformity of the Mesozoic, which indicate that dissolution is greatly influenced by unconformity (Figure 14a,b). Given the evolution pathway of pores under thermal compaction, the secondary porosity can be identified (Figure 15). The secondary porosity also exerts heterogeneous distribution at different regions in study area. The secondary pores are more abundant in regions that have been subjected to prolonged flushing by meteoric waters. Therefore, the regional unconformity exerts crucial control on secondary porosity, which in turn influence the reservoir quality.

The uplift of the basin was a depressure process of the strata, which provides conditions for the sand body rebound. The physical simulation experiment of sand rebound presented by Jiang (2004) showed that the maximum rebound volume of sand body caused by stratum uplift could reach 1% [55]. The preservation and increase of pore volume can provide favorable conditions for acidic fluid to flow through sandstone, and in turn promote dissolution.

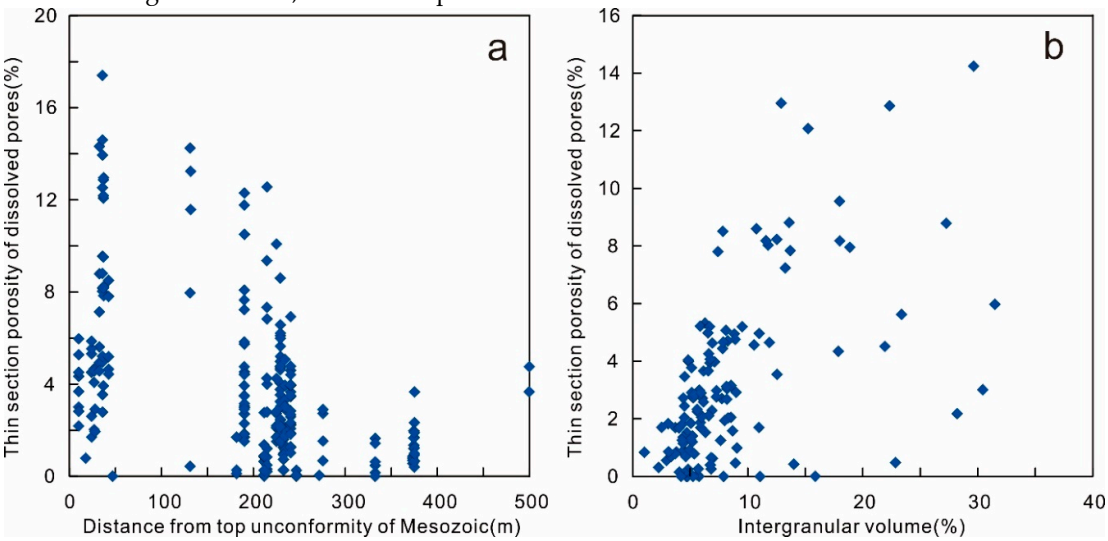

Figure 14. (a) Relationship between thin section porosity of dissolution pores and distance from top unconformity of Mesozoic; (b) Relationship between thin section porosity of dissolution pores and intergranular volume.

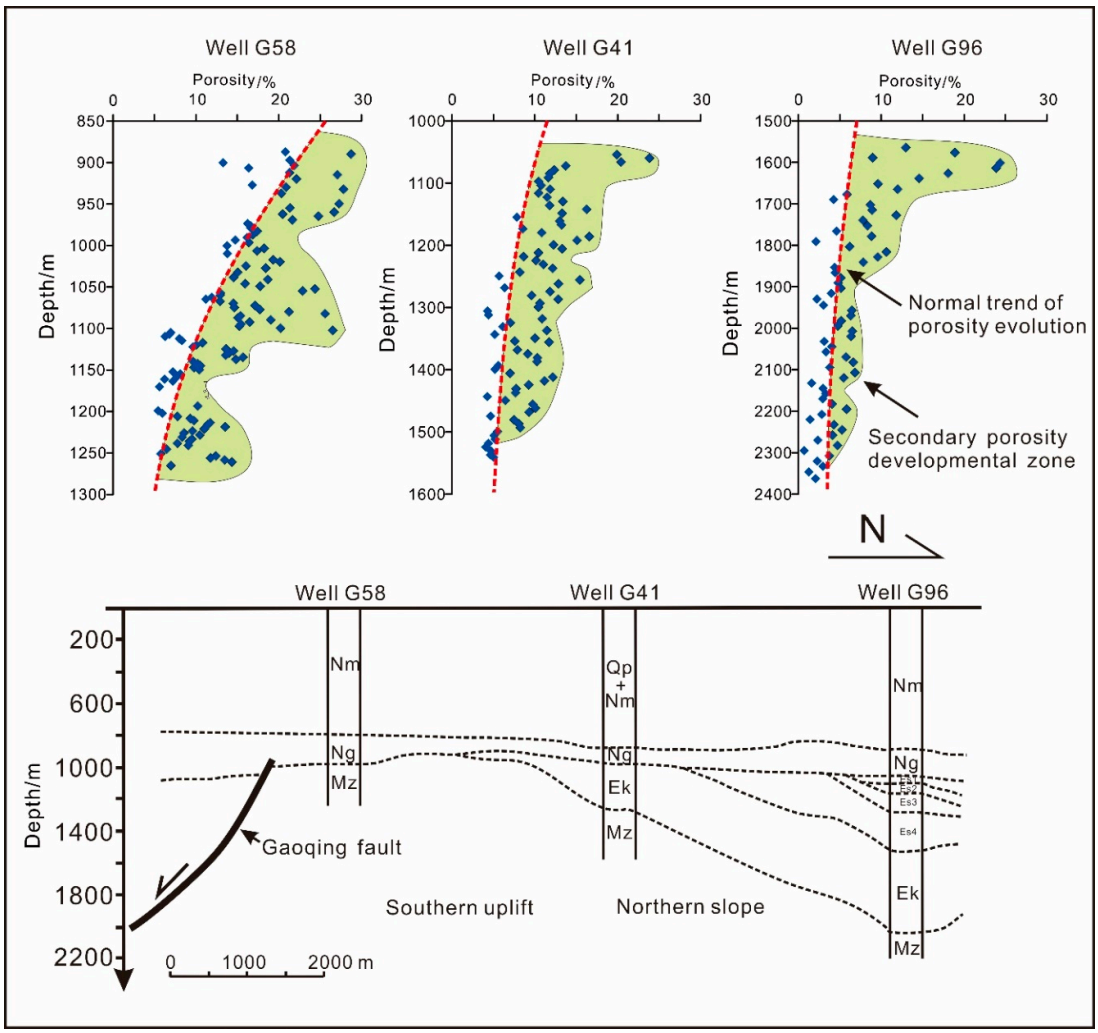

Figure 15. The extents and scales of secondary porosity at different regions in study area.

5.4. Fault Activity and Its Controls on Hydrocarbon Distribution

The activities of the Gaoqing fault and its derived faults induced micro-fractures in adjacent reservoir rocks. The fractures are the main pathways that connected meteoric water and deep-buried sandstones, and thus, increase the permeability by several orders of magnitude by meteoric flushing, which would greatly improve the seepage capacity and enhance the heterogeneity of reservoir rocks. In addition, as the main oil source fault of study area, the Gaoqing fault profoundly controls the hydrocarbon accumulation and migration in the study area [23]. According to the moving velocity analysis of seismic traces, the activity of Gaoqing fault started at Ek-Es4, and the intensity reached the peak at Es3-Es2 (Figure 16). After that, the intensity of fault activity gradually decreased. It can be seen that the Gaoqing fault remained active during hydrocarbon charging. Thus, the Gaoqing fault was served as the dominating vertical migrated pathway for hydrocarbon originated from source rocks in the downdropped block (Figure 17). The J_3m sandstone thickness with hydrocarbon indication and the height of oil column both show a strong negative correlation with the distance from the oil source fault (Figure 18). Therefore, the reservoir rocks closer to the Gaoqing fault are more likely to be enriched in oil and gas.

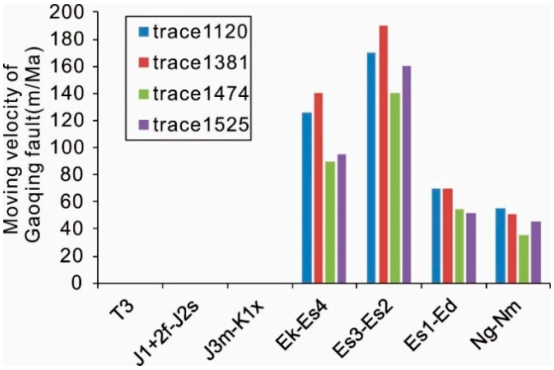

Figure 16. The moving velocity of the Gaoqing fault posed by seismic traces.

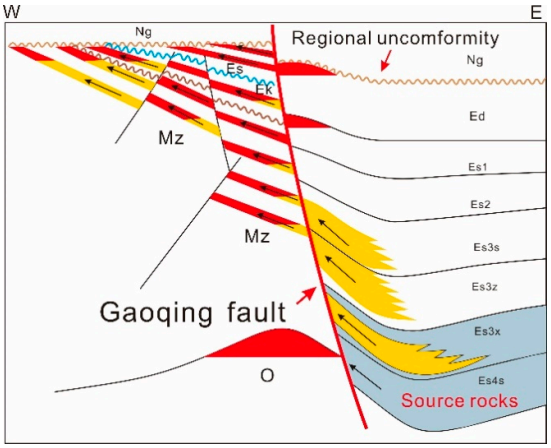

Figure 17. The hydrocarbon migration pattern in the study area.

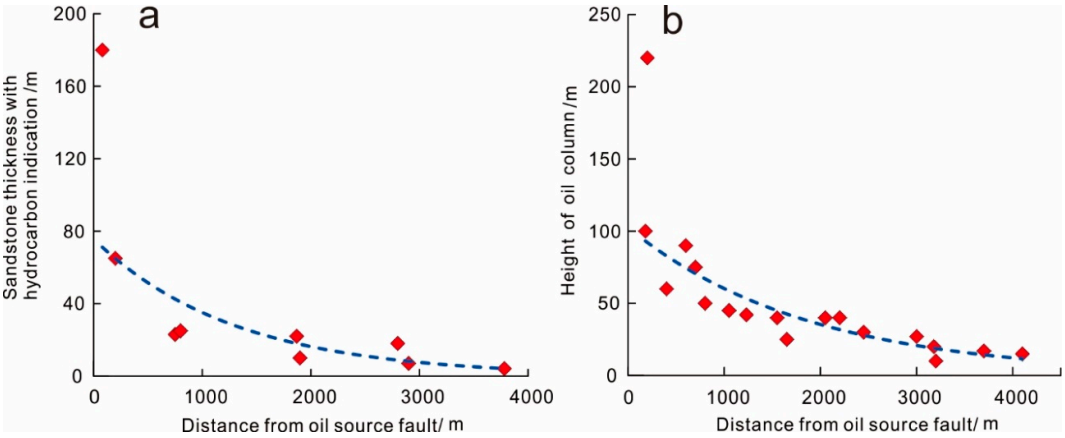

Figure 18. Relationship between hydrocarbon distribution and distance from oil source fault in the study area.

6. Conclusions

With the comprehensive analysis of petrographic characteristic, diagenesis and reservoir quality at macro and micro scales, this study provides important insight into the understanding of the controls and mechanism of the Upper Jurassic Mengyin Formation sandstones and valuable for the comprehensive reservoir characterization and reservoir properties prediction in the Dongying Depression.

During lengthy geological history, the sandstones of the Upper Jurassic Mengyin Formation experienced three burial and uplift episodes in basin evolution. Correspondingly, the diagenetic evolution sequence can be broadly related to three important phases. During early burial phase, sandstones were subjected to eogenetic carbonate cementation, which is believed to play an important role in original pores preservation and subsequent dissolution. Initial deep burial under high paleogeothermal gradient caused a significant porosity loss, which averaged out to about 20%. Uplift in the late Cretaceous resulted in meteoric flushing in Mengyin Formation sandstones, forming dissolved secondary pores of feldspar and carbonate cements accompanied with precipitation of kaolinite and syntaxial quartz crystals. Thin section porosity of dissolved pores shows a significant negative correlation with distance from top unconformity of the Mesozoic. Dissolution have been the most important porosity enhancing factor during reservoir quality evolution. The extensive compaction in sandstones also resulted in extremely low pore fluid flow, thus, the reaction products of dissolution cannot be removed, which would be precipitated as carbonate cements during a stable reburial phase. The mid-stage carbonate cements are generally well preserved in the sandstones, only minor cements are dissolved by organic rich acid from hydrocarbon charging, thus, they largely destroy the reservoir quality.

Due to the strong modifications by diagenesis and tectonics, the links between sedimentary setting and diagenetic processes have been weakened. Hence, the reservoir quality variations between different lithology are complicated and heterogeneous. The prediction of reservoir quality requires the basis of burial history (effective stress and temperature), uncomformity-related meteoric water flushing and fault activity. Among them, the main influential factor of reservoir quality is the burial pathway and compaction degree during the lengthy history. The present burial depth has a poor guidance on reservoir quality in these sandstones in Bohai Bay Basin of eastern China, which have undergone early deep burial under high paleogeothermal gradient.

Author Contributions: Investigation, Y.W.; Methodology, Y.Z.; Resources, Y.Z.; Supervision, S.Z.; Writing – original draft, Y.W.; Writing – review and editing, S.Y. All authors have read and agreed to the published version of the manuscript.

Funding: This study is sponsored by the China National Science and Technology Major Project (grant no. 2017ZX05009001).

Conflicts of Interest: The authors declare no conflict of interest.

References

1. Ajdukiewicz, J.M.; Lander, R.H. Sandstone reservoir quality prediction: The state of the art. *AAPG Bull*. **2010**, *94*, 1083–1091.
2. Taylor, T.R.; Giles, M.R.; Hathon, L.A.; Diggs, T.N.; Braunsdorf, N.R.; Birbiglia, G.V.; Kittridge, M.G.; Macaulay, C.I.; Espejo, I.S. Sandstone diagenesis and reservoir quality prediction: Models, myths, and reality. *Am. Assoc. Petroleum Geol. Bull*. **2010**, *94*, 1093–1132.
3. Morad, S.; Al-Aasm, I.S.; Nader, F.H.; Ceriani, A.; Gasparrini, M.; Mansurbeg, H. Impact of diagenesis on the spatial and temporal distribution of reservoir quality in the Jurassic Arab D and C members, offshore Abu Dhabi oilfield, United Arab Emirates. *GeoArabia* **2012**, *17*, 17–56.
4. Yuan, G.; Cao, Y.; Gluyas, J.; Li, X.; Xi, K.; Wang, Y.; Jia, Z.; Sun, P.; Oxtoby, N.H. Feldspar dissolution, authigenic clays, and quartz cements in open and closed sandstone geochemical systems during diagenesis: Typical examples from two sags in Bohai Bay Basin, East China. *AAPG Bull*. **2015**, *99*, 2121–2154.
5. Yuan, G.; Gluyas, J.; Cao, Y.; Oxtoby, N.H.; Jia, Z.; Wang, Y.; Li, X. Diagenesis and reservoir quality evolution of the Eocene sandstones in the northern Dongying Sag, Bohai Bay Basin, East China. *Mar. Pet. Geol*. **2015**, *62*, 77–89.
6. Xi, K.; Cao, Y.; Jahren, J.; Zhu, R.; Bjørlykke, K.; Haile, B.G.; Zheng, L.; Hellevang, H. Diagenesis and reservoir quality of the Lower Cretaceous Quantou Formation tight sandstones in the southern Songliao Basin, China. *Sediment. Geol*. **2015**, *330*, 90–107.
7. Perri, F.; Cirrincione, R.; Critelli, S.; Mazzoleni, P.; Pappalardo, A. Clay mineral assemblages and sandstone compositions of the Mesozoic Longobucco Group (north-eastern Calabria): Implication for burial history and diagenetic evolution. *Int. Geol. Rev*. **2008**, *50*, 1116–1131.

8. Luo, J.L.; Morad, S.; Salem, A.; Ketzer, J.M.; Lei, X.L.; Guo, D.Y.; Hlal, O. Impact of diagenesis on reservoir-quality evolution in fluvial and lacustrine-deltaic sandstones: Evidence from Jurassic and Triassic sandstones from the ordos basin, China. *J. Pet. Geol.* **2009**, *32*, 79–102.
9. Morad, S.; Al-Ramadan, K.; Ketzer, J.M.; De Ros, L.F. The impact of diagenesis on the heterogeneity of sandstone reservoirs: A review of the role of depositional facies and sequence stratigraphy. *AAPG Bull*. **2010**, *94*, 1267–1309.
10. Guo, X.; Liu, K.; He, S.; Song, G.; Wang, Y.; Hao, X.; Wang, B. Petroleum generation and charge history of the northern Dongying depression, Bohai Bay Basin, China: Insight from integrated fluid inclusion analysis and basin modelling. *Mar. Pet. Geol*. **2012**, *32*, 21–35.
11. Guo, S.; Tan, L.; Lin, C.; Li, H.; Lü, X.; Wang, H. Hydrocarbon accumulation characteristics of beach-bar sandstones in the southern slope of the Dongying Sag, Jiyang Depression, Bohai Bay Basin, China. *Pet. Sci*. **2014**, *11*, 220–233.
12. Henares, S.; Caracciolo, L.; Cultrone, G.; Fernandez, J.; Viseras, C. The role of diagenesis and depositional facies on pore system evolution in a triassic outcrop analogue (SE Spain). *Mar. Pet. Geol*. **2014**, *51*, 136–151.
13. Zhang, H.; Zhang, R.; Yang, H.; Shou, J.; Wang, J.; Liu, C.; Chen, G. Characterization and evaluation of ultra-deep fracture-pore tight sandstone re- servoirs: A case study of Cretaceous Bashijiqike Formation in Kelasu tectonic zone in Kuqa foreland basin, Tarim, NW China. *Pet. Explor. Dev.* **2014**, *41*, 158–167.
14. Zhou, Y.; Ji, Y.; Zhang, S.; Wan, L. Controls on reservoir quality of Lower Cretaceous tight sandstones in the Laiyang Sag, Jiaolai Basin, eastern China: Integrated sedimentologic, diagenetic and microfracturing data. *Mar. Pet. Geol*. **2016**, *76*, 26–50.
15. Lai, J.; Wang, G.; Wang, S.; Cao, J.; Li, M.; Pang, X.; Zhou, Z.; Fan, X.; Dai, Q.; Yang, L.; et al. Review of diagenetic facies in tight sandstones: Diagenesis, diagenetic minerals, and prediction via well logs. *Earth Sci. Rev.* **2018**,*185*, 234–258.
16. Nabawy, B.S.; Géraud, Y. Impacts of pore-and petro-fabrics, mineral composition and diagenetic history on the bulk thermal conductivity of sandstones. *J. Afr. Earth Sci*. **2015**, *115*, 21–24.
17. Cook, J.E.; Goodwin, L.B.; Boutt, D.F. Systematic diagenetic changes in the grain-scale morphology and permeability of a quartz-cemented quartz arenite. *AAPG Bull*. **2011**, *95*, 1067–1088.
18. Mozley, P.S.; Heath, J.E.; Dewers, T.A.; Bauer, S.J. Origin and heterogeneity of pore sizes in the Mount Simon sandstone and Eau Claire formation: Implications for multiphase fluid flow. *Geosphere* **2016**, *12*, 1341–1361.
19. Bjorlykke, K.; Jahren, J. Open or closed geochemical systems during diagenesis in sedimentary basins: Constraints on mass transfer during diagenesis and the prediction of porosity in sandstone and carbonate reservoirs. *AAPG Bull*. **2012**, *96*, 2193–2214.
20. Bjørlykke, K. Relationships between depositional environments, burial history and rock properties. Some principal aspects of diagenetic process in sedimentary basins. *Sediment. Geol*. **2014**, *301*, 1–14.
21. Higgs, K.E.; Crouch, E.M.; Raine, J.I. An interdisciplinary approach to reservoir characterization: An example from the early to middle eocene kaimiro formation, taranaki basin, New Zealand. *Mar. Pet. Geol.* **2017**, *86*, 111–139.
22. Wang, J.; Cao, Y.; Liu, K.; Liu, J.; Xue, X.; Xu, Q. Pore fluid evolution, distribution and water-rock interactions of carbonate cements in red-bed sandstone reservoirs in the Dongying Depression, China. *Mar. Pet. Geol.* **2016**, *72*, 279–294.
23. Wang, Y.; Yang, S.; Lu, Y.; Ma, B.; Zhao, Y.; Wang, Y. Characteristics and controlling factors of effective reservoirs of mesozoic low-permeability clastic rocks in Gaoqing region, Dongying depression, Bohai Bay basin, China. *Oil Gas Geol.* **2019**, *40*, 271–283 (in Chinese with English abstract).
24. Henares, S.; Caracciolo, L.; Viseras, C.; Fernandez, J.; Yeste, L.M. Diagenetic constraints on heterogeneous reservoir quality assessment: A Triassic outcrop analog of meandering fluvial reservoirs. *AAPG Bull*. **2016**, *100*, 1377–1398.
25. Gier, S.; Worden, R.H.; Johns, W.D.; Kurzweil, H. Diagenesis and reservoir quality of Miocene sandstones in the Vienna Basin, Austria. *Mar. Pet. Geol*. **2008**, *25*, 681–695.
26. Rustichelli, A.; Tondi, E.; Agosta, F.; Di Celma, C.; Giorgioni, M. Sedimentologic and diagenetic controls on pore-network characteristics of Oligocenee-Miocene ramp carbonates (Majella Mountain, central Italy). *AAPG Bull.* **2013**, *97*, 487–524.
27. Rossi, C.; Marfil, R.; Ramseyer, K.; Permanyer, A. Facies-related diagenesis and multiphase siderite cementation and dissolution in the reservoir sandstones of the Khatatba Formation, Egypt's Western Desert.

J. Sediment. Res. **2001**, *71*, 459–472.
28. Mansurbeg, H.; De Ros, L.F.; Morad, S.; Ketzer, J.M.; El-Ghali, M.A.K.; Caja, M.A.; Othman, R. Meteoric-water diagenesis in late Cretaceous canyon-fill turbidite reservoirs from the Espírito Santo Basin, eastern Brazil. *Mar. Pet. Geol*. **2012**, *37*, 7–26.
29. Yuan, G.; Cao, Y.; Zhang, Y.; Zhang, Y.; Gluyas, J. Diagenesis and reservoir quality of sandstones with ancient "deep" incursion of meteoric freshwater—An example in the Nanpu sag, Bohai Bay Basin, East China. *Mar. Pet. Geol*. **2017**, *82*, 444–464.
30. Changming, C.; Jiakuan, H.; Jingshan, C.; Xingyou, T. Depositional models of Tertiary rift basins, eastern China, and their application to petroleum prediction. *Sediment. Geol*. **1984**, *40*, 73–88.
31. Desheng, L. Geologic evolution of petroliferous basins on continental shelf of China. *AAPG Bull*. **1984**, *68*, 993–1003.
32. Zahid, M.A.; Chunmei, D.; Lin, C.; Gluyas, J.; Jones, S.; Zhang, X.; Muhammad, J.M.; Ma, C. Sequence stratigraphy, sedimentary facies and reservoir quality of es4s, southern slope of Dongying Depression, Bohai Bay Basin, East china. *Mar. Pet. Geol*. **2016**, *77*, 448–470.
33. Cao, Y.; Yuan, G.; Li, X.; Wang, Y.; Xi, K.; Wang, X.; Jia, Z.; Yang, T. Characteristics and origin of abnormally high porosity zones in buried Paleogene clastic reservoirs in the Shengtuo area, Dongying Sag, East China. *Pet. Sci*. **2014**, *11*, 346–362.
34. Wang, B.; Luo, S.; Chen, Y.; Wu, W. Numerical simulation of hydrocarbon generation, migration and accumulation in the boxing sag, Dongying Depression, Jiyang Subbasin. *Oil Gas Geol*. **2012**, *33*, 675–685, (in Chinese with English abstract).
35. Shen, B.; Huang, Z.; Liu, H.; Xu, C.; Yan, Z.; Chen, M. Geochemistry and origin of gas pools in the Gaoqing-Pingnan fault zone, Jiyang Depression. *Chin. J. Geochem*. **2007**, *26*, 446–454, doi:10.1007/s11631-007-0446-3.
36. Zhang, J.F.; Zhang, F.; Wu, H.; Xiang, X. Relationships between different strike activities of gaoqing fault and huagou gas reservoirs accumulation, jiyang depression. *Nat. Gas Geosci*. **2008**, 19, 356–361 (in Chinese with English abstract).
37. Wang, Y.; Yang, S.; Lu, Y.; Wang, X; Ma, B.; Zhao, Y. Evaluation method of low permeability reservoirs based on logging petrophysical facies identification: A case study of the upper member of Mengyin formation in Gaoqing area, Dongying depression. *J. China Univ. Min. Technol*. **2018**, *47*, 1264–1275, (in Chinese with English abstract).
38. Boggs, S. *Principles of Sedimentology and Stratigraphy;* Pearson Prentice Hall: Upper Saddle River, NJ, USA, 2006.
39. Bodnar. Revised equation and table for determining the freezing point depression of H2o-NaCl solutions. *Geochim. Cosmochim. Acta* **1993**, *57*, 683–684.
40. Folk, R.L. *Petrology of Sedimentary Rocks*; Hemphill Book Store: Hemphill, TX, USA, 1968; p. 170.
41. Anovitz, L.M.; Cole, D.R.; Rother, G.; Allard, L.F.; Jackson, A.J.; Littrell, K.C. Diagenetic changes in macro- to nano-scale porosity in the St. Peter Sandstone: An (ultra) small angle neutron scattering and backscattered electron imaging analysis. *Geochim. Cosmochim. Acta* **2013**, *102*, 280–305.
42. Anovitz, L.M.; Cole, D.R.; Jackson, A.J.; Rother, G.; Littrell, K.C.; Allard, L.F.; Pollington, A.D.; Wesolowski, D.J. Effect of quartz overgrowth precipitation on the multiscale porosity of sandstone: A (U)SANS and imaging analysis. *Geochim. Cosmochim. Acta* **2015**, *153*, 199–222.
43. Anovitz, L.M.; Cole, D.R. Characterization and analysis of porosity and pore structures. *Rev. Mineral. Geochem*. **2015**, *80*, 61–164.
44. Zou, C.; Zhu, R.; Liu, K.; Su, L.; Bai, B.; Zhang, X.; Yuan, X.; Wang, J. Tight gas sandstone reservoirs in China: Characteristics and recognition criteria. *J. Pet. Sci. Eng*. **2012**, *88–89*, 82–91.
45. Zhou, T.; Wu, C.; Shi, Z.; Wang, J.; Zhu, W.; Yuan, B.; Yang, D. Multi-Scale Quantitative Characterization of Pore Distribution Networks in Tight Sandstone by integrating FE-SEM, HPMI, and NMR with the Constrained Least Squares Algorithm. *Energies* **2019**, *12*, 3514.
46. Zhao, H.; Ning, Z.; Wang, Q.; Zhang, R.; Zhao, T.; Niu, T.; Zeng, Y. Petrophysical characterization of tight oil reservoirs using pressure-controlled porosimetry combined with rate-controlled porosimetry. *Fuel* **2015**, 154, 233–242.
47. Xiao, D.; Lu, Z.; Jiang, S.; Lu, S. Comparison and integration of experimental methods to characterize the full-range pore features of tight gas sandstone—A case study in Songliao basin of China. *J. Nat. Gas Sci. Eng*. **2016**, *34*, 1412–1421.
48. Higgs, K.E.; Zwingmann, H.; Reyes, A.G.; Funnell, R.H. Diagenesis, porosity evolution, and petroleum

emplacement in tight gas reservoirs, Taranaki basin, New Zealand. *J. Sediment. Res*. **2007**, *77*, 1003–1025.
49. Dutton, S.P.; Loucks, R.D. Diagenetic controls on evolution of porosity and permeability in lower Tertiary Wilcox sandstones from shallow to ultra-deep (200–6700 m) burial, Gulf of Mexico Basin, USA. *Mar. Pet. Geol*. **2010**, *27*, 69–81.
50. Houseknecht, D.W. Assessing the relative importance of compaction processes and cementation to reduction of porosity in sandstones. *Am. Assoc. Petrol. Geol. Bull*. **1987**, *71*, 633–642.
51. Beard, C.; Weyl, P.K. Influence of texture on porosity and permeability of un- consolidated sand. *Am. Assoc. Pet. Geol. Bull*. **1973**, *57*, 349–369.
52. English, K.L.; Redfern, J.; Corcoran, D.V.; English, J.M.; Yahia Cherif, R. Constraining burial history and petroleum charge in exhumed basins: New insights from the Illizi Basin. *Am. Assoc. Petroleum Geol. Bull*. **2016**, *100*, 623–655.
53. English, K.L.; English, J.M.; Bonnell, L.M.; Lander, R.H.; Hollis, C.; Redfern, J.; Guirdham, C.; Garnham, J.; Cherif, R.Y. Controls on reservoir quality in exhumed basins—an example from the ordovician sandstone, illizi basin, algeria. *Mar. Pet. Geol*. **2017**, *80*, 203–227.
54. Saïag, J.; Brigaud, B.; Portier, É.; Desaubliaux, G.; Bucherie, A.; Miska, S.; Pagel, M. Sedimentological control on the diagenesis and reservoir quality of tidal sandstones of the Upper Cape Hay formation (Permian, Bonaparte basin, Australia). *Mar. Mar. Pet. Geol*. **2016**, *77*, 597–624.
55. Jiang, Z.; Pang, X.; Jin, Z.; Guan, D.; Li, Y. Relationship between pore variation of reservoir and rebounding of sandstone during uplift and its application to the Daqing Oilfield. Earth Science: *J. China Univ. Geosci.* **2004**, *29*, 420–426, (in Chinese with English abstract).